Design, synthesis, solid-state and solution structures, non linear optical and computational studies of copper(II) complexes supported by variously substituted enantiomerically pure push-pull tetradentate Schiff base ligands

Salvador Celedon, Samia Kahlal, Jocelyn Oyarce, Olivier Cador, Vania Artigas, Mauricio Fuentealba, Isabelle Ledoux-Rak, David Carrillo, Jean-Yves Saillard, Jean-Rene Hamon, et al.

Design, synthesis, solid-state and solution structures, non linear optical and computational studies of copper(II) complexes supported by variously substituted enantiomerically pure push-pull tetradentate Schiff base ligands

Salvador Celedón[a],[*,1] Samia Kahlal[b], Jocelyn Oyarce[a], Olivier Cador[b], Vania Artigas[c], Mauricio Fuentealba[c], Isabelle Ledoux-Rak[d], David Carrillo[a], Jean-Yves Saillard[b], Jean-René Hamon[b],[*] Carolina Manzur[a],[*]

[a] *Laboratorio de Química Inorgánica, Instituto de Química, Facultad de Ciencias, Pontificia Universidad Católica de Valparaíso, Campus Curauma, Avenida Universidad 330, Valparaíso, Chile.*

[b] *Univ Rennes, CNRS, ISCR (Institut des Sciences Chimiques de Rennes) – UMR 6226, F-35000 Rennes, France.*

[c] *Laboratorio de Cristalografía, Instituto de Química, Facultad de Ciencias, Pontificia Universidad Católica de Valparaíso, Campus Curauma, Avenida Universidad 330, Valparaíso, Chile.*

[d] *Laboratoire Lumière, Matière et Interfaces, ENS Paris Saclay, UMR CNRS 9024, Institut d'Alembert, Centrale Supelec, 4 Avenue des Sciences, 91190 Gif-sur-Yvette, France.*

[1] *Present address: Instituto de Ciencias Naturales, Universidad de las Américas, Manuel Montt 948, Santiago, Chile.*

- Corresponding authors.

E-mail addresses: sceledn p@edu.udla.cl (S. Celedón), jean-rene.hamon@univ-rennes1.fr (J.-R. Hamon), cecilia.manzur@pucv.cl (C. Manzur).

Abstract

The synthesis, spectroscopic and structural characterization, optical and electrochemical properties and theoretical studies of a family of four new copper(II) complexes supported by a ferrocene-containing N_2O_2-tetradentate chiral Schiff base ligand derived from enantiomerically pure (1*R*,2*R*)-(−)-1,2-diaminocyclohexane are reported. The push-pull Cu(II) complexes were prepared following a one-pot three-component reaction involving the chiral half-unit (1*R*,2*R*)-Fc-C(=O)CH=C(CH_3)NH-*c*-C_6H_{10}-NH_2, copper acetate monohydrate and the appropriately 3-R,5-R'-substituted salicylaldehyde derivative in a 1:1:1 ratio (Fc = ferrocenyl; **3**: R = H, R' = Cl; **4**: R = H, R' = Br; **5**: R = R' = F; **6**: R = R' = NO_2), and isolated in 65-97 % yields as brown microcrystalline products. The characterization of the synthesized compounds were investigated through CHN elemental analysis, UV–vis, FT-IR, high-resolution mass spectrometry, and X-ray diffraction analysis in the case of the difluoro substituted complex **5** that was obtained in the form of single crystals. It crystallizes in the orthorhombic non-centrosymmetric space group $P2_12_12_1$, with two (*R*,*R*)-(−)-chiral carbon atoms in the structure. The four-coordinate Cu(II) metal ion adopts a slightly distorted square planar geometry. Magnetic properties of powdered samples have been investigated (2-300 K) and found consistent with a single isolated copper(II) ion (s=1/2). Cyclic voltammetry showed that the stronger the electron withdrawing effect of the 3,5-substituents, the more anodically shifted the oxidation potential ($E_{1/2}$) of the ferrocenyl moiety, following the order: 5-Cl < 5-Br < 3,5-F_2 < 3,5-$(NO_2)_2$. This trend is similar when considering the values of the second-order polarizabilities β of these compounds as measured using Harmonic Light Scattering (HLS) at 1.9 μm, confirming the increasing electron withdrawing effect evidenced by electrochemical studies as well as the conjugation between the electron donor ferrocenyl moiety and the different halogen or nitro substituents through the square planar copper Schiff base framework. Finally, DFT and TD-DFT calculations allow to rationalize the structure and properties of the complexes.

Keywords: copper; Chiral Schiff bases; DFT and TD-DFT calculations; Nonlinear optics; push-pull complexes; X-ray diffraction

1. Introduction

Schiff base ligands are known to benefiting from a large tunability including the rigidity/flexibility, denticity, and selective coordination sites [1,2]. Among them, tetradentate N_2O_2 Schiff bases derived from condensation of primary 1,2-diamines and two equivalents of carbonyl derivatives, are ubiquitous ligands as the N_2O_2 pocket endows it with strong metal coordination ability with virtually every metal ion in the periodic table under relative mild conditions [3-5]. Consequently, metal Schiff base complexes are valuable and important compounds which have found widespread applications in the field of synthetic chemistry [6,7], catalysis [8,9] materials science [10], nonlinear optics [11], sensing [12], and medicinal chemistry [13], to just name a few. On the other hand, chiral tetradentate salen-type Schiff base compounds which are usually accessed using optically pure 1,2-diamines [14,15], or in some instance from enantiopure salicylaldehyde derivatives [16], have also attracted great attention in the last few decades [17-19], displaying a lot of applications in asymmetric catalysis [20-27], medicine and biological activity [28-30].

On the other hand, implementing chirality opens the field to a variety of technologically important physical properties such as piezo/pyroelectricity and ferroelectricity [31], single-molecule/ion magnets [32,33] and magnetochiral effect [34], circularly-polarized luminescence (CPL) [35], as well as Second- Harmonic Generation (SHG) [36,37], that result from the crystallization in appropriate non-centrosymmetric space groups. In fulfilling this basic structural requirement, chiral Schiff base compounds containing π-conjugated framework with electron donor and acceptor groups to form a D-π-A push-pull system, have been shown to be good candidates for constructing second harmonic generation materials [38]. Coordination complexes of push-pull Schiff base ligands derived from chiral primary diamines do also form a promising and efficient class of nonlinear optical (NLO) molecular materials [39-41], showing sizeable solid-state NLO efficiencies, measured by the Kurtz-Perry method [42], with respect to standard urea. Chiral molecular inorganic-organic hybrid materials have recently been found to exhibit interesting second-order NLO properties in solution [43,44], measured by using Electric-Field-Induced Second Harmonic (EFISH) [45] or Harmonic Light Scattering (HLS) [46] techniques. The NLO behaviour of such Schiff base metal complexes in which the metal ion is a constituent of the polarizable bridge is due to the presence of low-energy and intense metal-to-ligand or ligand-to-metal charge-transfer transitions which are tunable by virtue of the nature, oxidation states, and coordination sphere of the metal centers [47].

Along this line, we have recently designed and prepared a series of four transition metal(II) complexes featuring a chiral unsymmetrically substituted N_2O_2 tetradentate Schiff base ligand, made of a donor ferrocenyl-functionalized redox-active β-keto-enamine linked to an electron withdrawing 5-nitrosalicylaldimine through the optically pure (1*R*,2*R*)-(−)-1,2-diaminocyclohexane [44]. Interestingly, all compounds showed good second-order NLO responses with β values ranging from 130 to 460 x 10^{-30} esu. Herein, we aim at exploring the electron withdrawing ability of the salicylidene substituent (halogeno and nitro groups) onto the NLO properties of a new family of copper(II) complexes featuring a related chiral D-π-A Schiff base platform. Thus, we wish to report the thorough investigation, including synthesis, analytical and spectroscopic characterization, and electrochemical behavior of the chiral neutral heterobimetallic Schiff base complexes [Cu{(1*R*,2*R*)-Fc-C(=O)CH=C(CH_3)N-*c*-C_6H_{10}-N=CH-(2-O,3-R,5-R'-C_6H_3)}] (Fc = Fe(η^5-C_5H_5) (η^5-C_5H_4), **3**: R = H, R' = Cl; **4**: R = H, R' = Br; **5**: R = R' = F; **6**: R = R' = NO_2; see formulas in Scheme 1). The crystal structure of the chiral 3,5-difluoro substituted derivative **5** is also disclosed. The second-order nonlinear polarizabilities of the inorganic-organic hybrid chromophores **3-6** have been measured in dichloromethane using the HLS technique at 1.9 μm. Finally, density functional theory (DFT) and time-dependent-DFT (TD-DFT) calculations were performed to better understand the electronic structure and optical properties as well as the nature of the bonds in all the products. When appropriate, data collected for **3-6** will be compared to those previously reported for the related Cu(II) complex **2** (R = H, R' = NO_2) [44].

2. Experimental

2.1. Materials and methods

All manipulations were carried out under a dinitrogen atmosphere using standard Schlenk techniques. The solvents were dried and distilled according to standard procedures [48]. Enantiomerically pure (1*R*,2*R*)-(−)-1,2-diaminocyclohexane, 2-hydroxy-5-chlorobenzaldehyde, 2-hydroxy-5-bromobenzaldehyde, 2-hydroxy-3,5-difluorobenzaldehyde, 2-hydroxy-3,5-dinitrobenzaldehyde and copper(II) acetate monohydrate were purchased from Aldrich and used without further purification. The chiral half-unit (1*R*,2*R*)-(−)-Fc-C(=O)CH=C(CH_3)NH-*c*-C_6H_{10}-NH_2 (**1**) [49], and the Cu(II) complex **2** [44] were synthesized according to literature procedures. Solid-state FT-IR spectra were recorded on a Perkin-Elmer Model 1600 FT-IR spectrophotometer with KBr disks in the 4000 to 400 cm^{-1} range. Electronic

spectra were obtained with a SHIMADZU UV-1800 spectrophotometer. High resolution electrospray ionization mass spectra (ESI-MS) were obtained at the Centre Regional de Mesures Physiques de l'Ouest (CRMPO, Université de Rennes, France) with a Bruker MAXI 4G spectrometer. Elemental analyses were conducted on a Thermo-Finnigan Flash EA 1112 CHNS/O analyzer by the Microanalytical Service of the CRMPO. The temperature dependences of the magnetizations for powdered samples of **2-6** have been measured with a Quantum design MPMS-XL5 SQUID magnetometer operating between 2 and 300 K, with an applied magnetic field of 2 kOe below 20 K and of 10 kOe above 20 K. Diamagnetic corrections were applied by using Pascal's constants [50]. Cyclic voltammetry (CV) measurements were performed with a CH instruments/ model Ch604E potentiostat, using a standard three-electrode setup with a glassy carbon working electrode, platinum wire auxiliary electrode, and Ag/AgCl as the reference electrode. Dimethylformamide (DMF) solutions were 1.0 mM in the compound under study and 0.1 M in the supporting electrolyte *n*-$Bu_4N^+PF_6^-$ with voltage scan rate of 100 mV s^{-1}. Ferrocene was added as an internal standard at the end of each experiment.

*2.2. Synthesis of complexes **3-6** general procedure*

To a Schlenk tube containing a stirred solution of half-unit **1** (250 mg, 0.683 mmol) in ethanol (10 mL) was added dropwise the desired substituted salicylaldehyde dissolved in ethanol (5 mL) and the stirring was continued for 15 min. Then, a solution of copper(II) acetate monohydrate (138 mg, 0.683 mmol) in ethanol (5 mL) was added and the reaction medium was refluxed for 1 h, giving a microcrystalline precipitate. Upon cooling to room temperature, the solid material was collected by filtration, washed with cold methanol and diethyl ether (2 × 5 mL), and dried under vacuum.

*2.2.1. Data for [Cu{(1R,2R)-Fc-C(=O)CH=C(CH_3)N-c-C_6H_{10}-N=CH-(2-O,5-Cl-C_6H_3)}] (**3**)*

The synthesis of this brown microcrystalline complex was carried out using 2-hydroxy-5-chlorobenzaldehyde (109 mg, 0.683 mmol). Yield: 288 mg, 74.5 %. Anal. Calcd for $C_{27}H_{27}ClCuFeN_2O_2$ (566.37 g mol^{-1}): C, 57.26; H, 4.81; N, 4.95. Found: C, 56.44; H, 4.64; N, 4.79. ESI MS (*m*/*z*) calcd for $C_{27}H_{27}N_2O_2{}^{35}Cl^{56}Fe^{63}Cu$: 565.04009, found: 565.0406 $[M]^+$. FT-IR (KBr, cm^{-1}): 3095 (m), 3057 (m) (C−H arom), 2934 (m), 2858 (m) (C−H aliph), 1636 (vs) (C⋯O), 1603 (m), 1525 (s) (C⋯C) and/or (C⋯N), 727 (w) (C−H), 664 (w) (C−Cl), 517 (m) (Cu−O), 483 (w) (Cu−N).

*2.2.2. Data for [Cu{(1R,2R)-Fc-C(=O)CH=C(CH$_3$)N-c-C$_6$H$_{10}$-N=CH-(2-O,5-Br-C$_6$H$_3$)}] (**4**)*

The synthesis of this brown microcrystalline complex was carried out using 2-hydroxy-5-bromobenzaldehyde (140 mg, 0.683 mmol). Yield: 406 mg, 97.4 %. Anal. Calcd for $C_{27}H_{27}BrCuFeN_2O_2$ (610.82 g mol^{-1}): C, 53.09; H, 4.46; N, 4.59. Found: C, 52.93; H, 4.41; N, 4.55. ESI MS (*m*/*z*) calcd for $C_{27}H_{27}N_2O_2{}^{79}Br^{56}Fe^{63}Cu$: 608.98958, found: 608.9899 $[M]^+$. FT-IR (KBr, cm^{-1}): 3096 (m), 3057 (m) (C−H arom), 2933 (m), 2858 (m) (C−H aliph), 1635 (vs) (C⋯O), 1593 (s), 1521 (s) (C⋯C) and/or (C⋯N), 713 (w) (C−H), 651 (w) (C−Br), 514 (w) (Cu−O), 483 (w) (Cu−N).

*2.2.3. Data for [Cu{(1R,2R)-Fc-C(=O)CH=C(CH$_3$)N-c-C$_6$H$_{10}$-N=CH-(2-O,3,5-F$_2$-C$_6$H$_2$)}] (**5**)*

The synthesis of this brown microcrystalline complex was carried out using 2-hydroxy-3,5-difluorobenzaldehyde (111 mg, 0.683 mmol). Yield: 388 mg, 81.3 %. X-ray quality crystals were obtained by slow diffusion of diethyl ether into a solution of complex **5** in a 1:1 mixture of dimethylformamide and ethanol. Anal. Calcd for $C_{27}H_{26}CuF_2FeN_2O_2$ (567.90 g mol^{-1}): C, 57.10; H, 4.61; N, 4.93. Found: C, 57.15; H, 4.45; N, 4.80. ESI MS (*m*/*z*) calcd for $C_{27}H_{26}N_2O_2F_2{}^{56}Fe^{63}Cu$: 567.06022, found: 567.0603 $[M]^+$; (*m*/*z*) calcd for $C_{27}H_{26}N_2O_2F_2Na^{56}Fe^{63}Cu$: 590.04999, found: 590.0508 $[M + Na]^+$. FT-IR (KBr, cm^{-1}): 3087 (m), 3022 (m) (C−H arom), 2926 (m), 2853 (m) (C−H aliph), 1635 (s) (C⋯O), 1572 (m), 1550 (m) (C⋯C) and/or (C⋯N), 1120 (m) (C−F), 742 (w) (C−H), 508 (w) (Cu−O), 436 (vw) (Cu−N).

*2.2.4. Data for [Cu{(1R,2R)-Fc-C(=O)CH=C(CH$_3$)N-c-C$_6$H$_{10}$-N=CH-(2-O,3,5-(NO$_2$)$_2$-C$_6$H$_2$)}] (**6**)*

The synthesis of this brown microcrystalline complex was carried out using 2-hydroxy-3,5-dinitrobenzaldehyde (149 mg, 0.683 mmol). Yield: 280 mg, 65.2 %. Anal. Calcd for $C_{27}H_{26}CuFeN_4O_6$ (621.92 g mol^{-1}): C, 52.15; H, 4.21; N, 9.01. Found: C, 52.64; H, 4.27; N, 9.00. ESI MS (*m*/*z*) calcd for $C_{27}H_{26}N_4O_6{}^{56}Fe^{63}Cu$: 621.04922, found: 621.0497 $[M]^+$. FT-IR (KBr, cm^{-1}): 3092 (m), 3057 (m) (C−H arom), 2931 (s), 2861 (m) (C−H aliph), 1645 (s) (C⋯O), 1604 (s), 1559 (s) (C⋯C) and/or (C⋯N), 1499 (vs) asym (N⋯O), 1326 (vs) sym (N⋯O), 706 (w) (C−H), 526 (w) (Cu−O), 448 (vw) (Cu−N).

2.3. X-ray Crystal Structure Determination

A well-shaped clear light red single crystal of compound **5** was mounted on top of glass fibers in a random orientation. Diffraction data were collected at 296(2) K on a Bruker D8

QUEST diffractometer equipped with a bidimensional CMOS Photon100 detector, using graphite monochromated Mo-Kα radiation (λ = 0.71073 Å). The diffraction frames were integrated using the APEX2 package [51], and were corrected for absorptions with SADABS. The structure was solved by direct methods using the OLEX 2 program [52]. The structure was then refined with full-matrix least-square methods based on F^2 (*SHELXL-97*) [53]. All non-hydrogen atoms were refined with anisotropic atomic displacement parameters. All hydrogen atoms were included in their calculated positions, assigned fixed isotropic thermal parameters and constrained to ride on their parent atoms. A summary of the details about crystal data, collection parameters and refinement are documented in Table 1, and additional crystallographic details are in the CIF file. ORTEP views were drawn using OLEX2 software [52].

CCDC-2270914 contains the supplementary crystallographic data for this paper. These data can be obtained free of charge via http://www.ccdc.cam.ac.uk/conts/retrieving.html (or from the Cambridge Crystallographic Data Centre, 12, Union Road, Cambridge CB2 1EZ, UK; fax: +44 1223 336033).

Table 1 Crystallographic data, details of data collection and structure refinement parameters for compound **5**.

	5
Empirical Formula	$C_{27}H_{26}CuF_2FeN_2O_2$
Formula mass, g mol^{-1}	567.89
Collection T, K	296(2)
crystal system	Orthorhombic
space group	$P2_12_12_1$
a (Å)	9.1902(4)
b (Å)	21.0411(9)
c (Å)	24.5335(11)
V (Å^3)	4744.1(4)
Z	8
D_{calcd} (g cm^{-3})	1.590
Crystal size (mm)	0.500 x 0.101 x 0.074
Crystal color	clear light red
Crystal description	Plate
F(000)	2328
abs coeff (mm^{-1})	1.552
θ range (°)	2.106 to 26.429
range h,k,l	-11/11, -26/26, -30/30
No. total refl.	181460
No. unique refl.	9757
Comp. θ_{max} (%)	99.9
Max/min transmission	0.9275/0.6339
Data/Restraints/Parameters	9757/0/633
Final R [$I>2\sigma(I)$]	R_1 = 0.0276 wr_2 = 0.0634
R indices (all data)	R_1 = 0.0374 wr_2 = 0.0680
Goodness of fit / F^2	1.078
Largest diff. Peak/hole (eÅ^{-3})	0.300/-0.196

2.4. Kurtz-Perry Second harmonic powder tests and HLS Measurements

In order to check the non-centrosymmetric character of the molecular organization within the crystal structures, second harmonic generation (SHG) measurements were made using a modified Kurtz and Perry powder technique [42], using a nanosecond Nd^{3+} :YAG laser operating at 1.06 μm, a Potassium dihydrogenophosphate (KDP) powder being used as the reference material. Powders are deposited on a glass plate, and SHG scattered from the samples are collected using the same set-up as for the HLS experiment described below.

For the first-order hyperpolarizabilities (β) measurements of the Schiff-base chromophores **3**-**6**, HLS [46] was performed using the same 10 Hz repetition-rate nanosecond Nd^{3+}:YAG laser pumping a high-pressure molecular hydrogen cell in order to produce a fundamental wavelength of 1.91 μm by stimulated Raman scattering. The measurements were carried out with solutions of **3**-**6** in dichloromethane (see Table 5 for concentrations used). This solvent is chosen for its high transparency at 1.91 μm and for its ability to dissolve molecules **3**-**6** at concentrations reaching 10^{-2} M if necessary. A concentrated (10^{-2} M) solution of ethyl violet (its octupolar β value being 170 x 10^{-30} esu at 1.91 μm) in the same solvent was used as external reference. By using a wavelength of 1.91 μm, the harmonics at 955 nm remains far from any resonance of the molecules, then preventing from the contribution of possible two-photon fluorescence emission to the HLS signal. We verified the absence of any wide-band two-photon fluorescence by checking that no HLS signal could be detected for wavelengths other than 955 nm. The experimental setup and details of data analysis have been described previously [54].

2.5. Computational details

DFT calculations were carried out using the ADF2020 package [55,56], incorporating the relativistic scalar corrections via the ZORA Hamiltonian [57], and employing the PBE0 functional [58,59] and the TZ2P basis set [60], together with Grimme's empirical DFT-D3(BJ) corrections for dispersion forces [61]. The optimized geometries were characterized as true minima on the potential energy surface using vibrational frequency calculations (no imaginary values). The UV-vis transitions were calculated by means of TD-DFT calculations on the optimized geometries, at the same level of theory.

3. Results and discussion

3.1. Synthesis and characterization

The chiral bimetallic Schiff-base complexes **3**-**6**, along with the known relative **2** [44], were prepared via a one-pot three-component procedure starting from the tridentate proligand **1**, copper(II) acetate monohydrate and the desired substituted salicylaldehyde derivative, in a molar ratio of 1:1:1, in refluxing ethanol for 1 h (Scheme 1). Complexes **3**-**6** precipitated directly from the reaction mixture and were collected by filtration as microcrystalline solids isolated in good to excellent yields ranging from 65 to 97 % (see Experimental Section). X-ray quality crystals were only obtained for the 3,5-difluoro derivative **5**. All attempts to grow crystals suitable for X-ray diffraction study proved to be unsuccessful for the four other complexes **2**-**4** and **6**. Brown Compounds **3**-**6** are found to be air-stable solids that are soluble in CH_2Cl_2, DMF and DMSO.

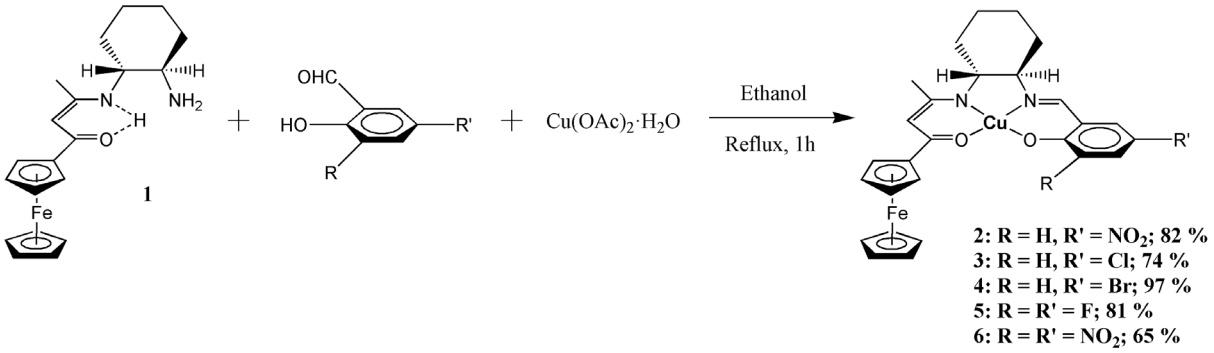

Scheme 1. Synthesis of the chiral Schiff base Cu(II) complexes **2**-**6**.

The bulk purity of the newly prepared complexes **3**-**6** was determined through elemental analysis, and their composition and formulation were established from FT-IR, UV-vis, and single crystal X-ray crystallography for the heterobimetallic species **5** (see below). In addition, HRMS positive ESI spectra showed the expected isotopic distribution for the molecular ion peaks $[M]^+$ for the four compounds, along with the sodium aggregate $[M + Na]^+$ for **5** (see Experimental Section and Figs. S1-S4 in Supplementary Material).

The solid-state FT-IR spectra (KBr disk) of compounds **3**-**6** are depicted in Fig. S5 (SM), along with selected major IR wavenumbers gathered in Table S1 (SM). They are all quite similar showing the same main characteristic features of the organic Schiff base skeleton [49].

Those are (i) a strong band at 1635-1645 cm^{-1} due to the ν(C⋯O) stretching mode, (ii) a set of medium to strong intensity absorptions in the 1604-1572 cm^{-1} and 1559-1521 cm^{-1} regions attributed to ν(C⋯N) and ν(C⋯C) stretching vibrations, respectively and (iii) a strong deformation mode of the C−H bonds observed in the 706-742 cm^{-1} range. Additionally, vibration bands appearing in the Far-IR spectra of **3-6** at 517, 514, 508, and 526 cm^{-1} and at 483, 483, 436, and 448 cm^{-1}, can be associated to the Cu-O and Cu-N stretching vibrations, respectively [62]. Those abovementioned IR data fully agree with those previously registered for complex **2** (Table S1, SM) [44], and clearly indicate that in the four new compounds under investigation herein, the tetradentate Schiff base ligands are coordinated to the centered Cu(II) metal ion through the amino and azomethine nitrogens, and carbonyl and phenoxo oxygens. The dianionic N_2O_2 coordination mode is further confirmed by X-ray crystallography (see below). Finally, the different substituents of the salicylidene ring are highlighted by their specific stretching vibration: ν(C−Cl) at 664 cm^{-1} for **3**, ν(C−Br) at 651 cm^{-1} for **4**, ν(C−F) at 1120 cm^{-1} for **5**, and ν_{asym} and ν_{sym}(N⋯O) at 1499 and 1326 cm^{-1}, respectively, for **6** [63].

The electronic absorption spectra of the chiral Schiff base Cu(II) complexes **3**-**6** in the UV-vis region were measured in dimethylformamide (DMF) (Figs. 1 and S6-S8, SM). The spectral data are collected in Table 2 with those reported for the related compound **2**. According to the TD-DFT calculations described below, the higher energy bands observed at 354-370 nm are assigned to π-π* transition due to the imine groups and aromatic rings, thus belonging to ligand-to-ligand charge transfer (LLCT) transitions. The absorption bands of lower energy showing maxima in the 433-470 nm range are a mixture of Fe→π* metal-to-ligand charge transfer (MLCT) with π→Fe ligand-to-metal charge transfer (LMCT). Lastly, the low-energy absorption bands in the visible region at 645, 663 and 658 nm for **3**, **4** and **5**, respectively, are tentatively assigned to MLCT transitions. Participation of some d-d transitions could not, however, be excluded [64,65].

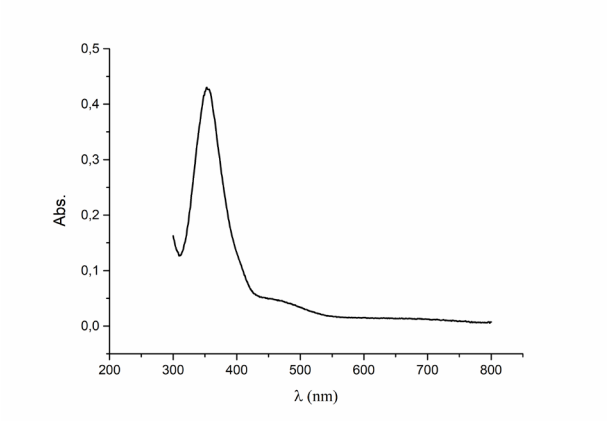

Fig. 1 UV-Vis spectrum of the chiral Schiff base Cu(II) complex **5** measured in DMF solution at 20 °C.

Table 2 UV-vis absorption data for compounds **2-6**.

Compd.	λ / nm (Log ε) (DMF)
2[a]	362 (4.36) 473 (3.15)
3	369 (3.90) 463 (3.26) 645 (2.27)
4	370 (3,76) 461 (3.14) 663 (1.87)
5	354 (4.33) 470 (3.35) 658 (2.82)
6	357 (4.48) 433 (3.92)

[a] from ref. [44].

The magnetic properties of powdered samples of the Schiff base Cu(II) compounds **2** and **5** have been recorded as a function of the temperature and magnetic field. The temperature variations of $\chi_M T$ for both compounds are represented in Fig. 2. The room temperature values of $\chi_M T$, with χ_M the molar magnetic susceptibility and T the temperature in Kelvin, are equal to 0.42 and 0.43 cm^3 K mol^{-1} respectively. These values are in good agreement with what is expected for isolated Cu(II) spin (s=1/2) [66]. With such Curie constants, average effective Zeeman factors of 2.12 and 2.14 can be extracted. $\chi_M T$ remains quasi constant on cooling down

to 50 K and slightly decreases at lower temperatures for both compounds to reach 0.36 cm^3 K mol^{-1} at 2 K. Such behaviour can be due to the presences of small intermolecular antiferromagnetic interactions.

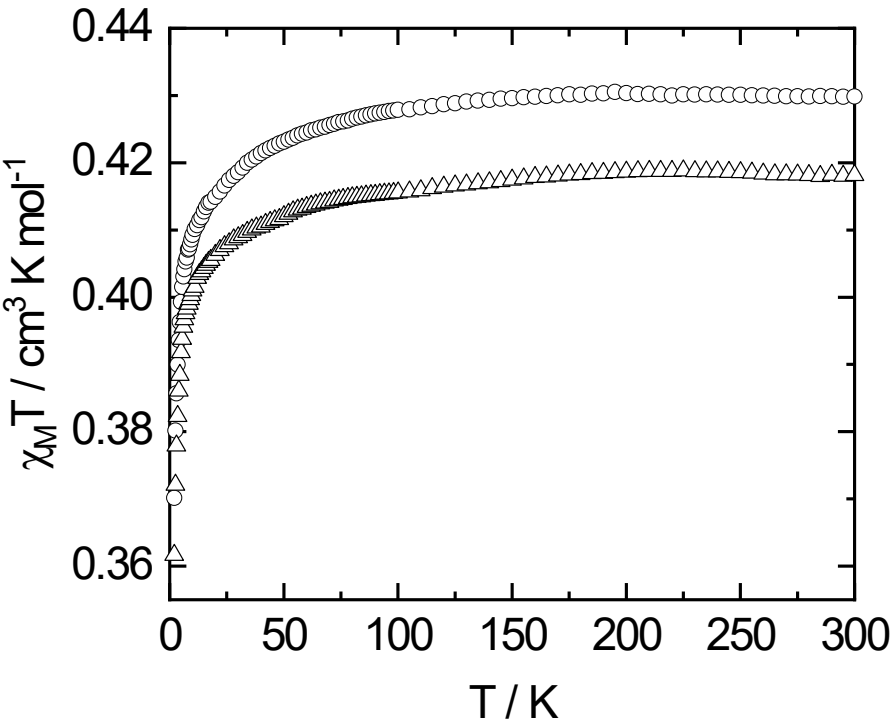

Fig. 2 Temperature variations of $\chi_M T$ for compounds **2** (triangles) and **5** (circles).

*3.2. Crystal structure description of the chiral Schiff base Cu(II) complex **5***

Crystals of the chiral Schiff base Cu(II) complex **5** suitable for X-ray crystallography were grown by slow diffusion of diethyl ether into a solution of the compound in DMF/MeOH (1:1) mixture. The molecular structure of **5** is shown in Fig. 3. Bond distances and angles for the first copper(II) coordination sphere are provided in Table 3, whereas the other relevant bond distances and angles are gathered in Table S2 (SM). Complex **5** crystallizes in the orthorhombic non-centrosymmetric space group $P2_12_12_1$ with two crystallographically nonequivalent molecules (**5A**, **5B**) found in the asymmetric unit. Compound **5** consists of a ferrocenyl unit linked to a copper(II)-centered N_2O_2 unsymmetrical macroacyclic Schiff base framework doubly substituted with fluorine group. The cyclohexane-diyl ring adopts a chair conformation and the ferrocenyl unit features a typical linear η^5-Fe-η^5 sandwich structure, with metrical parameters in agreement with a Fe(II) oxidation state [67]. The cyclopentadienyl rings are

parallel and staggered by ~ 27° (Table S3, SM). In the crystal packing, the molecules are loosely connected to one another through weak intermolecular hydrogen bonds (Fig. S9 and Table S4, SM).

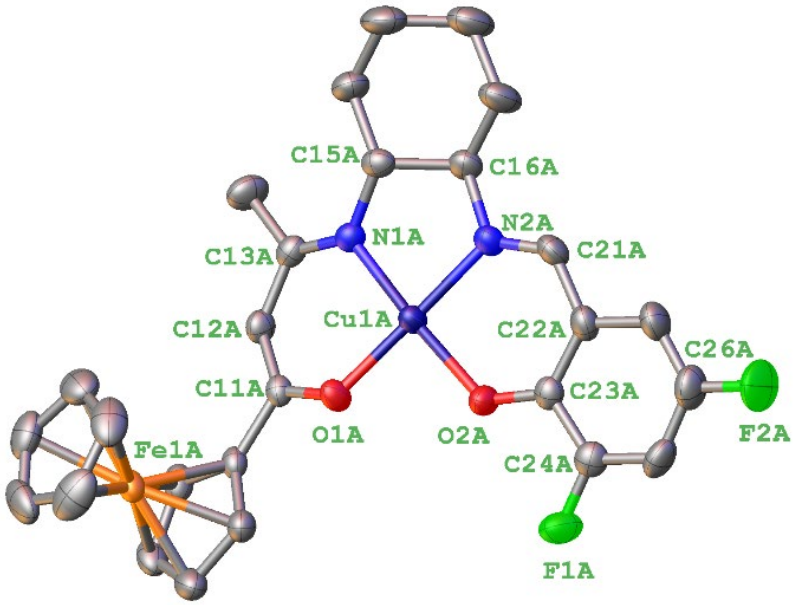

Fig. 3 Molecular structure of complex **5** (molecule A) with numbering scheme for selected atoms. Hydrogens are omitted for clarity. Thermal ellipsoids are drawn at 50 % probability.

Table 3 Selected bond distances (Å) and angles (°) for the first Cu(II) coordination sphere of compound **5**.

	5A	**5B**
Cu(1)-O(1)	1.896(3)	1.896(3)
Cu(1)-O(2)	1.922(3)	1.924(3)
Cu(1)-N(1)	1.952(3)	1.957(3)
Cu(1)-N(2)	1.940(3)	1.941(3)
O(1)-Cu(1)-N(2)	174.27(14)	174.60(14)
O(2)-Cu(1)-N(1)	168.22(14)	165.11(14)
O(1)-Cu(1)-N(1)	95.38(13)	95.98(13)

O(1)-Cu(1)-O(2)	87.44(11)	86.57(12)
O(2)-Cu(1)-N(2)	92.59(13)	92.99(13)
N(1)-Cu(1)-N(2)	85.74(14)	85.82(14)

Complex **5** contains a four-coordinate copper(II) metal ion located in the N_2O_2-inner sphere of the two-fold deprotonated Schiff base ligand, being coordinated to amido and imine nitrogens and to carbonyl and phenolato oxygens (Fig. 3). This dianionic tetradentate binding mode leads to the formation of a six-, five-, six-membered chelate ring arrangement around the central Cu(II) ion, with the nitrogen and oxygen atoms occupying mutually *trans* positions and forming O-Cu -N bite angles of 92-95° (Table 3). The copper(II) atom adopts a slightly distorted square planar geometry with a τ_4 index value of 0.124 for **5A** over 0.143 for the **5B** counterpart (τ_4 = 0 for a perfect square planar geometry) [68]. The central Cu(II) atom deviates from the N_2O_2 basal plane by 0.050(2) Å in **5A** and 0.080(2) Å in **5B**, leading to angular summations of 361.15 and 361.36°, respectively. This deviation from an idealized square planar geometry is, however, less pronounced than that observed with the related achiral 3,5-difluorinated Schiff base ligand in which the rigid *o*-phenylene acts as the linker in place of the more flexible 1,2-cyclohexane-diyl in **5** (τ_4 index = 0.212, sum of angles = 363.72°) [69]. Of peculiar interest, the [Cu(N_2O_2)] core is part of a bowed chelate Schiff base scaffold with curvature angles of 170.67(12) and 165.32(11)° between the two central carbon atoms of the 6-membered chelate rings, C(12) and C(22), and the central copper atom. Similar curvatures have also been observed for the Ni(II) counterpart [44].

On the other hand, the bond lengths and angles in the first coordination sphere of the centered copper(II) ions (Table 3) are very similar to those measured for related Cu(II) complexes featuring acyclic unsymmetrical Schiff-base ligands [65,69]. The two six-membered heterometallacycles are planar with O-C, C-C and C-N bond lengths ranging between reported values for single and double bonds (see Table S2, SM) [70]. The plane of the substituted cyclopentadienyl ring of the donor ferrocenyl fragment makes a weak dihedral angle of 13.34(13)° in **5A** and 8.79 (14)° in **5B** with the mean plane of the heterometallacycle to which it is attached to, suggesting a significant delocalization of the electron density throughout the whole framework.

3.3. Electrochemical study

In order to determine the electronic effects of the various electron withdrawing substituents (**3**: 5-Cl; **4**: 5-Br; **5**: 3,5-F_2; **6**: 3,5-$(NO_2)_2$) on the electrochemical behavior of the bimetallic Schiff base complexes **3-6**, cyclic voltammetry (CV) experiments were performed in DMF solution containing 0.1 M *n*-$Bu_4N^+PF_6^-$ as supporting electrolyte, at room temperature. Scans were restricted between +0.30 and +1.00 V. The cyclovoltammograms of the ferrocenyl unit of the four compounds are depicted in Fig. 4 and their respective formal electrode potentials $E_{1/2}$ (*vs*. AgCl) are listed in Table 4. These redox processes arising from the monoelectronic oxidation of the ferrocenyl moiety, are chemically reversible with current ratio i_{pa}/i_{pc} equals to unity. The anodic to cathodic peak-to-peak (ΔE_p) separations are, however, significantly greater than the ideal value of 60 mV for a fully reversible one-electron process. This may result from a combination of low solubility of some compounds, uncompensated solution resistance and presumably slow electron-transfer kinetics [71].

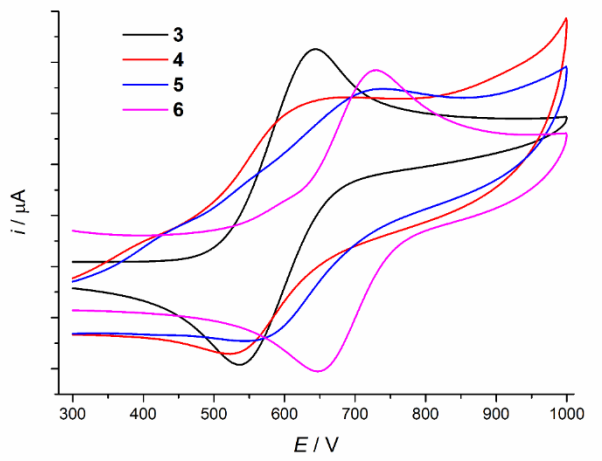

Fig. 4 Cyclic voltammograms of complexes **3-6** recorded in DMF containing 0.1 M *n*-$Bu_4N^+PF_6^-$ at $T = 298$ K with a sweep rate $v = 0.1$ V s^{-1}, reference electrode Ag/AgCl.

Table 4 Formal electrode potentials and peak-to-peak separations for the Fe^{II}/Fe^{III} redox processes exhibited by compounds **3-6**.[a]

Compd.	$E_{1/2}$/V	ΔE_p/mV
3	0.59	108
4	0.61	165

5	0.65	177
6	0.69	82
Cp_2Fe	0.49	76

[a]Recorded in DMF containing 0.1 M *n*-$Bu_4N^+PF_6^-$ at T = 298 K with a sweep rate v = 100 mV s^{-1}, reference electrode Ag/AgCl.

The redox potentials are in accordance with the electron withdrawing ability of the substituents borne by the salicylidene core of the complexes. In each case, the $E_{1/2}$ values are anodically shifted (100-200 mV) with respect to that of free ferrocene (Table 4), thus featuring the electron withdrawing ability of the Schiff base side-chain. This anodic shift also suggests that there is a strong interaction between the donor ferrocenyl moiety and the acceptor fragment, resulting from a favored electron delocalization in the [$Cu(N_2O_2)$] Schiff base platform mediated by the open-shell d^9 configuration of the central copper(II) metal ion. As expected from previous work [69], the nitro group exerts a stronger electron withdrawing effect than the fluorine one, as the anodic shift vs. that of the ferrocene/ferricenium redox couple ($\Delta E_{1/2}$) is greater for the 3,5-dinitro derivatives **6** than for its 3,5-difluoro counterpart **5**, with $\Delta E_{1/2}$ values of +200 and +160 mV, respectively. Interestingly, in complex **2** bearing only one nitro substituent at the 5-position of the salicylidene ring, the $\Delta E_{1/2}$ value is found to be +140 mV [44], close to the anodic shift observed for the 3,5-difluoro derivative **5**, and similar to that measured for the *o*-phenylene linked analogue ($\Delta E_{1/2}$ = 135 mV) [69]. The CV data obtained here are in accordance with our previous observations within this family of bimetallic macroacyclic unsymmetrical Schiff base complexes whatever the diimine spacer employed (1,2-ethylene-diyl, *o*-phenylene or 1,2-cyclohexane-diyl) [44,69 ,72].

3.4. Quadratic NLO Studies

All compounds have been submitted to the Kurtz and Perry Powder test [42] at 1.06 µm. Among them, only crystal powder of compound **5** exhibited a SHG signal reaching only 20% of that of the reference KDP material. This small value can be due to the fact that the compound strongly absorbs in the visible, resulting in a strong reduction of the second harmonic intensity at 532 nm as compared to that from the transparent KDP powder. This SHG emission confirms the non-centrosymmetric character of the $P2_12_12_1$ space group as identified by the X-Ray studies reported above.

The hyperpolarizabilities β of compounds **2-6** are reported in Table 5. The electron withdrawing character seems to increase according to the following order: Br < Cl < NO_2< 3,5-$(NO_2)_2$ < 3,5-F_2. As compared to the ranking found via electrochemical studies, the electron withdrawing characters of 3,5-F_2 and 3,5-$(NO_2)_2$ derivatives are inverted, the difluoro compound being apparently more efficient than the dinitro one. The same trend appears when comparing bromide and chloride derivatives, but with a smaller relative difference.

Table 5 Second-order polarizabilities β of compounds **2-6** as measured in CH_2Cl_2 by HLS at 1.9 μm.

Compound	Concentration (mol.L^{-1})	β (10^{-30} esu)	β_0 (10^{-30} esu)
2[a]	4.61 10^{-3}	205	145
3	1.78 10^{-3}	150	72
4	1.80 10^{-3}	135	62
5	1.80 10^{-3}	330	151
6	1.79 10^{-3}	230	181

[a] from ref. [44].

However, from the UV-visible spectral data reported in Table 2, the halogenated compounds display a long-wavelength band around 650 nm which does not exist in the nitro compounds. This transition plays a significant role in the enhancement of β values via resonance effect with the harmonic wavelength. We must then consider the dispersion-free intrinsic hyperpolarizability value (β_0) of these compounds, that can be calculated using a two-state model as proposed in Ref [73], giving $\beta_0 = \beta_{1.91}(1-(\lambda_{max}/\lambda)^2)(1-(2\lambda_{max}/\lambda)^2)$, where λ_{max} is the experimental optical absorption maximum and λ is the fundamental wavelength of the laser. In Table 5, we have reported these calculated β_0 values by taking as λ_{max} the highest λ values reported in Table 2. As a consequence, the hyperpolarizabilities of the halogen derivatives are strongly reduced with respect to their corresponding values at 1.91, and the ranking of their electron-withdrawing character becomes almost the same as that found from electrochemical studies, i.e.: 5-Br < 5-Cl < 5-NO_2 < 3,5-F_2 < 3,5-$(NO_2)_2$. In fact, the slightly lower β_0 value found for the bromide derivative as compared to the chlorinated one reflects the

electronegativity difference between Cl and Br, the former being stronger than the latter one. Lastly, one can note that the nonlinear responses found for the chiral series **2-6** under investigation are similar to those we previously determined for the related non-chiral Cu(II) Schiff base complexes (β = 200-270 x 10^{-30} esu) In which the (1R,2R)-1,2-cyclohexane-diyl spacer has been substituted for 1,2-ethane-diyl or o-phenylene linker [69,72,74]. This suggests that introducing a chiral backbone is not a sufficient tool to increase the NLO properties, at least in solution. Incorporation of functional groups enables to generate supramolecular architectures through hydrogen bonds would favor a better organization of the chromophoric entities, thus optimizing the NLO response of Schiff base complexes [75].

3.5. Computational investigations

Density functional theory (DFT) calculations at the PBE0/TZ2P/D3(BJ) level were performed to optimize the geometries of compounds **2-6** (see section 2.5. Computational Details). Their optimized structures are shown in Fig. 5. Selected computed data are provided in Table S5 (SM). Molecules **5A** and **5B** were optimized taking their X-ray structures as starting geometries. Whereas we were expecting two identical optimized geometries (*i.e.,* one unique energy minimum in vacuum), the two optimized structures were found to differ in the rotation angle of the ferrocenyl angle around the C-C bond linking it to the rest of the molecule. In the optimized **5A** molecule, the rotation brings one H atom of the "free" Cp ring at a distance of 2.56 Å from one of the fluorine atom (Fig. S10, SM). This feature is not present in the experimental structure of **5A**, nor in the optimized geometry of **5B** (F…H > 5 Å). Beside of that, the metrical data of both optimized structures are very close (see Table S5, SM) and their energy difference (0.7 kcal/mol) is not different from zero at our level of accuracy. Although our calculations probably overestimate somewhat the strength of the F…H interaction, they illustrate the almost free rotation of the ferrocenyl substituent around its linking bond. Since no F…H contact is present in the X-ray structures of **5**, only the optimized structure of **5B** is shown in Figure 5 and considered thereafter.

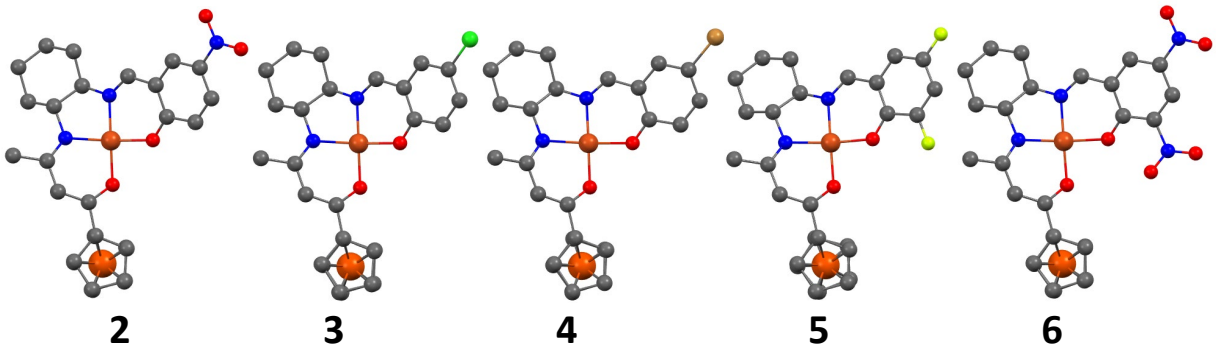

Fig. 5 DFT-optimized geometries of compounds **2**-**6**. Hydrogen atoms omitted for clarity.

The five complexes in Fig. 5 exhibit similar structures, with very similar metrical data (Table S5, SM). It is of note that the dihedral angle between the C_6 aromatic ring and CuN(1)N(2)O(1)O(2) mean planes falls into the narrow 14°-19° range for all the complexes, indicating related conjugation effects between these two parts of the molecule.

The Kohn-Sham spinorbital diagram of complex **3** is shown in Fig. 6. Those of the other complexes are quite similar. Their level ordering is provided in Fig. S11 (SM). As expected, the nitro-substituted complexes **2** and **6** have their orbitals lying at slightly lower energy than their halogen-substituted relatives **3**-**5**. The two lowest unoccupied spinorbitals of **3** are the α and β components of a π*(ligand) combination which is mainly located on the salicylidene ring, N(2) and O(2). The vacant β counterpart of the α spinorbital containing the unpaired Cu(II) electron can be identified as mixed within the two levels situated right above (147β and 148β). As expected, they exhibit $3d_{x2-y2}$(Cu) character with non-negligible metal-ligand antibonding admixture. The two highest SOMOs of **3** are the α and β components of a π(ligand) combination. The 3d(Fe) levels of the ferrocenyl substituent (the so-called "t_{2g}" set) are situated below. The two highest contain non-negligible admixture from the ligand π-type system (Fig. 6), illustrating some electronic communication between Fe and the substituted salicylidene ring. The 3d(Cu) levels, including the spinorbital containing the Cu^{II} unpaired electron, are situated far below those of Fe parentage. As a consequence, the oxidation of compounds **2**-**6** is found to occur at the Fe^{II} center, in line with the electrochemical experiments (see above).

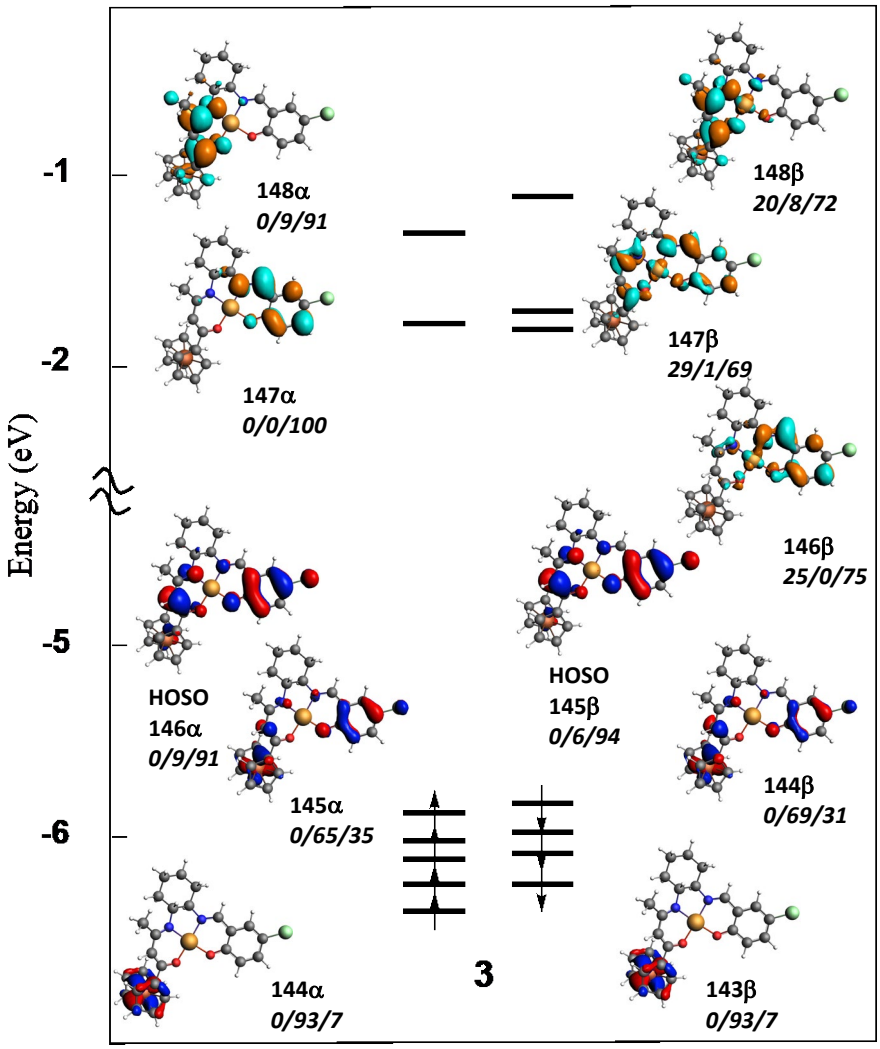

Fig. 6 Frontier Kohn-Sham spinorbital diagram of **3**. The spinorbital localizations (in %) are given in the order Cu/Fe/ligands.

Consistently, for all the complexes the oxidized (cationic) species is found to have a triplet ground state, which can be viewed as having two unpaired electrons, one on the Cu^{II} center with some (weak) delocalization on its first neighbors, and the other one on the oxidized Fe^{III}. This is exemplified by the spin density plot of $\mathbf{3}^{+}$ shown in Fig. S12 (SM).There is a qualitative agreement between the computed ionization energies of **2**-**6** (6.21, 6.68, 6.67, 6.77 and 7.18 eV, respectively) and their experimental $E_{1/2}$ values (Table 4).

TD-DFT calculations were also performed on compounds **2**-**6** for indexing their absorption bands. The corresponding simulated spectra are shown in Fig. S13 (SM). The agreement with experiment is only qualitative, but the shape of the spectra is satisfyingly

reproduced. The simulated spectra are separated in two groups according to the nature of their substituent(s) on the salicylidene ring (nitro group(s): **2** and **6**; halogen(s): **3**-**5**). The more intense high-energy band is of LLCT character with minor FeLCT admixture. The second more intense band is of large ferrocenyl-to-substituted salicylidenyl charge transfer nature with some FeLCT admixture. The weak absorption experimentally observed around 650 nm for **3**-**5** could not be reproduced by TD-DFT.

4. Conclusions

In summary, we have designed, synthesized and fully characterized a series of copper(II) complexes supported with various substituted chiral Schiff base ligands, employing the enantiomerically pure (1*R*,2*R*)-(−)-1,2-diaminocyclohexane as the chiral source for the construction of the N_2O_2-tetradentate macroacyclic ligand. The neutral bimetallic Cu(II) complexes are formed of a central [Cu(ONNO)] core surrounded by a ferrocenyl donor group and a salicylidene ring substituted with either 5-nitro, 5-chloro, 5-bromo, 3,5-difluoro or 3,5-dinitro electron withdrawing groups, yielding interesting D-π-A push-pull chromophores. Their electrochemical, linear, and second-order nonlinear optical properties have been thoroughly investigated. X-ray diffraction study of the 3,5-difluorosubstituted complex showed that it crystallizes in the orthorhombic non-centrosymmetric space group $P2_12_12_1$ with two (R,R) chiral carbon atoms in the molecule, the four-coordinate Cu(II) metal ion adopts a slightly distorted square planar geometry, and the [Cu(N_2O_2)] core is inserted into a bowed unsymmetrical Schiff base scaffold. The nature and strength of the electron withdrawing group borne by the salicylidene ring affect the oxidation potential ($E_{1/2}$) of the ferrocenyl moiety with an anodic -shift in the following order: 5-Cl < 5-Br < 5-NO_2 < 3,5-F_2 < 3,5-$(NO_2)_2$. The stronger the electron withdrawing effect, the more positively shifted the $E_{1/2}$ value. An almost similar ranking is inferred from nonlinear optical measurements, bromide showing a slightly weaker withdrawing character than chlorine in the conjugate Schiff base, this ordering being more compatible with the smaller electronegativity of bromide as compared to chlorine. Therefore, we evidenced a nice convergence between electrochemical and NLO data. To add to the experimental characterization, DFT- and TD-DFT-based theoretical analyses allow interpretation of their observed spectroscopic, structural and electronic features. We are aiming at exploring the organization of such Schiff base containing NLO-phores in polymeric films for the further elaboration of NLO materials.

Declaration of Competing Interest

The authors declare that they have no known competing financial interests or personal relationships that could have appeared to influence the work reported in this paper.

Credit authorship contribution statement

Salvador Celedón: investigation, Methodology, software. Samia Kahlal: investigation, software. Jocelyn Oyarce: investigation, Methodology. Olivier Cador: investigation, Formal analysis, Writing –original draft. Vania Artigas: investigation, software. Mauricio Fuentealba: Formal analysis, Writing –original draft. Isabelle Ledoux-Rak: investigation, Formal analysis, Writing –original draft. David Carrillo: Conceptualization, Writing –review & editing. Jean-Yves Saillard: Formal analysis, Writing –original draft, Writing –review & editing. Jean-René Hamon: Data curation, conceptualization, Writing –original draft, Writing –review & editing. Carolina Manzur: Project administration, Funding acquisition, Conceptualization, Writing – review & editing.

Data Availability

The data that support the findings of this study are available in the supplementary material associated with this article.

Acknowledgments

We thank P. Jehan (CRMPO, Rennes) for helpful assistance with HRMS measurements. This research was performed as part of the Chilean-French International Research Project "IRP-CoopIC" 2022-2026. Financial support from the Fondo Nacional de Desarrollo Científico y Tecnológico (FONDECYT), Chile (grant 1090310) and FONDEQUIP EQM130154 and EQM120095], the Vicerrectoría de Investigación y Estudios Avanzados, Pontificia Universidad Católica de Valparaíso, Chile (VRIEA-PUCV), the Centre National de la Recherche Scientifique (CNRS) and the Université de Rennes is gratefully acknowledged. S.C. thanks VRIEA-PUCV for a postdoctoral financing.

Supplementary materials

Supplementary material associated with this article can be found, in the online version, at doi:

References

[1] L. Fabbrizzi, Beauty in Chemistry: Making Artistic Molecules with Schiff Bases, J. Org. Chem. 85 (2020) 12212-12226. DOI: 10.1021/acs.joc.0c01420

[2] W. Qin, S. Long, M. Panunzio, S. Biondi, Schiff bases: A short survey on an evergreen chemistry tool, Molecules 18 (2013) 12264-12289. DOI: 10.3390/molecules181012264

[3] M. Calligaris, G. Nardin, L. Randaccio, Structural aspects of metal complexes with some tetradentate Schiff bases, Coord. Chem. Rev. 7 (1972) 385-403. https://www.sciencedirect.com/science/article/pii/S0010854500800181

[4] R. Hernandez-Molina, A. Mederos, Acyclic and Macrocyclic Schiff Base Ligands, in: J.A. McCleverty, T.J. Meyer (Eds.), Comprehensive Coordination Chemistry II, Elsevier Pergamon, Oxford, UK, 2004, Vol. 1.19, pp. 411-458.

[5] C. Boulechfar, H. Ferkous, A. Delimi, A. Djedouani, A. Kahlouche, A. Boublia, A.S. Darwish, T. Lemaoui, R. Verma, Y. Benguerba, Schiff bases and their metal Complexes: A review on the history, synthesis, and applications, Inorg. Chem. Commun. 150 (2023) 110451. DOI: 10.1016/j.inoche.2023.110451

[6] K.T. Hylland, I. Gerz, D.S. Wragg, S. Oien-Odegaard, M. Tilset, The Reactivity of Multidentate Schiff Base Ligands Derived from Bi- and Terphenyl Polyamines towards M(II) (M=Ni, Cu, Zn, Cd) and M(III) (M=Co, Y, Lu), Eur. J. Inorg. Chem. (2021) 1869-1889. DOI: 10.1002/ejic.202100170

[7] X. Liu, C. Manzur, N. Novoa, S. Celedon, D. Carrillo, J.-R. Hamon, Multidentate unsymmetrically-substituted Schiff bases and their metal complexes: Synthesis, functional materials properties, and applications to catalysis, Coord. Chem. Rev. 357 (2018) 144-172. DOI: 10.1016/j.ccr.2017.11.030

[8] P.G. Cozzi, Metal-Salen Schiff base complexes in catalysis: practical aspects, Chem. Soc. Rev. 33 (2004) 410-421. DOI: 10.1039/b307853c

[9] R. Malav, S. Ray, Carbon-carbon cross coupling reactions assisted by Schiff base complexes of Palladium, cobalt and copper: A brief overview, Inorg. Chim. Acta 551 (2023) 121478. DOI: 10.1016/j.ica.2023.121478

[10] C. Freire, M. Nunes, C. Pereira, D.M. Fernandes, A.F. Peixoto, M. Rocha, Metallo(salen) complexes as versatile building blocks for the fabrication of molecular materials and devices with tuned properties, Coord. Chem. Rev. 394 (2019) 104-134. DOI: 10.1016/j.ccr.2019.05.014

[11] Z. Fatima, H.A. Basha , S.A. Khan, A Review: An Overview on third-order nonlinear optical and optical limiting properties of Schiff Bases, J. Mol. Struct. (2023) DOI: 10.1016/j.molstruc.2023.136062

[12] M.Z. Alam, S.A. Khan, A review on Rhodamine-based Schiff base derivatives: synthesis and fluorescent chemo-sensors behaviour for detection of Fe^{3+} and Cu^{2+} ions, J. Coord. Chem. 76 (2023) 371-402 and references cited therein. doi.org/10.1080/00958972.2023.2183852

[13] A. Erxleben, Transition metal salen complexes in bioinorganic and medicinal chemistry, Inorg. Chim. Acta 472 (2018) 40-57. DOI: 10.1016/j.ica.2017.06.060

[14] Y.L. Bennani, S. Hanessian, trans-1,2-Diaminocyclohexane Derivatives as Chiral Reagents, Scaffolds, and Ligands for Catalysis: Applications in Asymmetric Synthesis and Molecular Recognition, Chem. Rev. 97 (1997) 3161-3195. DOI: 10.1021/cr9407577

[15] D. Lucet, T. Le Gall, C. Mioskowski, The Chemistry of Vicinal Diamines, Angew. Chem. Int. Ed. 37 (1998) 2580-2627. DOI: 10.1002/(SICI)1521-3773(19981016)37:19<2580::AID-ANIE2580>3.0.CO;2-L

[16] M. Chollet-Krugler, S. Tomasi, P. Uriac, L. Toupet, P. van de Weghe, Preparation and characterization of copper(II) and nickel(II) complexes of a new chiral salen ligand derived from (+)-usnic acid, Dalton Trans. (2008) 6524-6526. DOI: 10.1039/b811589c

[17] R.S. Downing, F.L. Urbach, The Circular dichroism of square-planar, tetradentate Schiff base chelates of copper(II), J. Am. Chem. Soc. 91 (1969) 5977-5983. DOI: 10.1021/ja01050a009

[18] A. Pasini, M. Gullotti, R. Ugo, Optically active complexes of Schiff bases. Part 4. An analysis of the circular-dichroism spectra of some complexes of different coordination

numbers with quadridentate Schiff bases of optically active diamines, J. Chem. Soc. Dalton Trans. (1977) 346-356. DOI: 10.1039/DT9770000346

[19] G. B. Roy, Synthesis and study of physico-chemical properties of a new chiral Schiff base ligand and its metal complex, Inorg. Chim. Acta 362 (2009) 1709-1714. DOI: 10.1016/j.ica.2008.08.009

[20] T. Katsuki, Some Recent Advances in Metallosalen Chemistry, Synlett (2003) 0281-0297. DOI: 10.1055/s-2003-37101

[21] J.F. Larrow, E.N. Jacobsen, Asymmetric Processes Catalyzed by Chiral (Salen)Metal Complexes, Top. Organomet. Chem. 6 (2004) 123-152. DOI: 10.1007/b11772

[22] L. Canali, D.C. Sherrington, Utilisation of homogeneous and supported chiral metal(salen) complexes in asymmetric catalysis, Chem. Soc. Rev. 28 (1999) 85-93. DOI: 10.1039/A806483K

[23] C. Baleizão, H. Garcia, Chiral Salen Complexes: An Overview to Recoverable and Reusable Homogeneous and Heterogeneous Catalysts, Chem. Rev. 106 (2006) 3987-4043. DOI: 10.1021/cr050973n

[24] S. Shaw, J.D. White, Asymmetric Catalysis Using Chiral Salen-Metal Complexes: Recent Advances, Chem. Rev. 119 (2019) 9381-9426. DOI: 10.1021/acs.chemrev.9b00074

[25] Y.-C. Yuan, M. Mellah, E. Schulz, O.R.P. David, Making Chiral Salen Complexes Work with Organocatalysts, Chem. Rev. 122 (2022) 8841-8883. DOI: 10.1021/acs.chemrev.1c00912

[26] E. Schulz, Chiral Cobalt-Salen Complexes: Ubiquitous Species in Asymmetric Catalysis, Chem. Rec. 21 (2021) 427-439. DOI: 10.1002/tcr.202000166

[27] A. Gualandi, C.M. Wilson, P.G. Cozzi, Stereoselective reactions with chiral Schiff base metal complexes, CHIMIA Int. J. Chem. 71 (2017) 562-567. DOI: 10.2533/chimia.2017.562

[28] S. Jos, N.R. Suja, Chiral Schiff base ligands of salicylaldehyde: A versatile tool for medical applications and organic synthesis-A review, Inorg. Chim. Acta 547 (2023) 121323. DOI: 10.1016/j.ica.2022.121323

[29] A. Soroceanu, A. Bargan, Advanced and Biomedical Applications of Schiff-Base Ligands and Their Metal Complexes: A Review, Crystals 12 (2022) 1436. DOI: 10.3390/cryst12101436

[30] X.-Q. Zhou, Y. Li,D.-Y. Zhang, Y. Nie, Z.-J. Li,W. Gu, X. Liu, J.-L. Tian, S.-P. Yan, Copper complexes based on chiral Schiff-base ligands: DNA/BSA binding ability, DNA cleavage activity, cytotoxicity and mechanism of apoptosis, Eur. J. Med. Chem. 114 (2016) 244-256. DOI: 10.1016/j.ejmech.2016.02.055

[31] K.M. Ok, E.O. Chi, P.S. Halasyamani, Bulk characterization methods for non-centrosymmetric materials: secondharmonic generation, piezoelectricity, pyroelectricity, and ferroelectricity, Chem. Soc. Rev. 35 (2006) 710-717. DOI: 10.1039/b511119f

[32] J. Long, Luminescent Schiff-Base Lanthanide Single-Molecule Magnets: The Association Between Optical and Magnetic Properties, Front. Chem. 7 (2019) 63. DOI: 10.3389/fchem.2019.00063

[33] D.-P. Li, T.-W. Wang, C.-H. Li, D.-S. Liu, Y.-Z. Li, X.-Z. You, Single-ion magnets based on mononuclear lanthanide complexes with chiral Schiff base ligands [Ln(FTA)$_3$L] (Ln = Sm, Eu, Gd, Tb and Dy), Chem. Commun. 46 (2010) 2929-2931. DOI: 10.1039/b924547b

[34] C. Train, M. Gruselle, M. Verdaguer, The fruitful introduction of chirality and control of absolute configurations in molecular magnets, Chem. Soc. Rev. 40 (2011) 3297-3312. DOI: 10.1039/c1cs15012j

[35] M. Savchuk, S. Vertueux, T. Cauchy, M. Loumaigne, F. Zinna, L. Di Bari, N. Zigon, N. Avarvari, Schiff-base [4]helicene Zn(II) complexes as chiral emitters, Dalton Trans. 50 (2021) 10533-10539. DOI: 10.1039/d1dt01752g

[36] A. Miniewicz, S. Bartkiewicz, E. Wojaczynska, T. Galica, R. Zalesny, R. Jakubas, Second harmonic generation in nonlinear optical crystals formed from propellane, J. Mater. Chem. C 7 (2019) 1255-1262. DOI: 10.1039/C8TC05268A

[37] T. Zhao, S. Ji, D. Zhong, F. Teng, S. Ullah, S. Hu, J. Tang, B. Teng, Synthesis, growth and characterization of N, N-dimethyl-4-[2-(2-quinolyl) vinyl] aniline (DADMQ): An SHG material for NLO applications, Optik 224 (2020) 165323. DOI: 10.1016/j.ijleo.2020.165323

[38] W. Tan, J. Gao, J. Guan, X. Bi, Y. Tang, C. Zheng, T. Yan, C. Zhang, Synthesis, characterization and theoretical calculations of four chiral Schiff base materials for second

harmonic generation applications, J. Mol. Struct. 1269 (2022) 133868. DOI: 10.1016/j.molstruc.2022.133868

[39] G. Lenoble, P.G. Lacroix, J.-C. Daran, S. Di Bella, K. Nakatani, Syntheses, Crystal Structures, and NLO Properties of New Chiral Inorganic Chromophores for Second-Harmonic Generation, Inorg. Chem. 37 (1998) 2158-2165. DOI: 10.1021/ic970481w

[40] F. Averseng, P.G. Lacroix, I. Malfant, F. Dahan, K. Nakatani, Synthesis, crystal structure and solid state NLO properties of a new chiral bis(salicylaldiminato)nickel(II) Schiff-base complex in a nearly optimized solid state environment, J. Mater. Chem. 10 (2000) 1013-1018. DOI: 10.1039/a910244m

[41] L. Rigamonti, A. Forni, E. Cariati, G. Malavasi, A. Pasini, Solid-State Nonlinear Optical Properties of Mononuclear Copper(II) Complexes with Chiral Tridentate and Tetradentate Schiff Base Ligands, Materials 12 (2019) 3595. DOI: 10.3390/ma12213595

[42] S.K. Kurtz, T.T. Perry, A Powder Technique for the Evaluation of Nonlinear Optical Materials, J. Appl. Phys. 39 (1968) 3798-3813. DOI: jap/article/39/8/3798/5301

[43] P. Matozzo, A. Colombo, C. Dragonetti, S. Righetto, D. Roberto, P. Biagini, S. Fantacci, D. Marinotto, A Chiral Bis(salicylaldiminato)zinc(II) Complex with Second-Order Nonlinear Optical and Luminescent Properties in Solution, Inorganics 8, (2020) 25. DOI: 10.3390/inorganics8040025

[44] S. Celedón, P. Hamon, V. Artigas, M. Fuentealba, S. Kahlal, I. Ledoux-Rak, D. Carrillo, J.-Y. Saillard, C. Manzur, J.-R. Hamon, Experimental and Theoretical Evaluation of Four NLO-Active Divalent Transition Metal Complexes Supported by an Enantiomerically Pure Tetradentate Schiff Base Ligand, Eur. J. Inorg. Chem. (2022) e202200478. DOI: 10.1002/ejic.202200478

[45] B.F. Levine, C.G. Bethea, Molecular hyperpolarizabilities determined from conjugated and nonconjugated organic liquids, Appl. Phys. Lett. 24 (1974) 445-447. DOI: 10.1063/1.1655254

[46] R.W. Terhune, P.D. Maker, C.M. Savage, MEASUREMENTS OF NONLINEAR LIGHT SCATTERING, Phys. Rev. Lett. 14 (1965) 681-684. DOI: 10.1103/PhysRevLett.14.681

[47] M.G. Humphrey, T. Schwich, P.J. West, M.P. Cifuentes, M. Samoc, Nonlinear Optical Properties of Coordination and Organometallic Complexes, in: J. Reedijk, K.

Poeppelmeier (Eds.), Comprehensive Inorganic Chemistry II, Elsevier, Oxford, UK, 2013, vol. 8, pp. 781-835.

[48] W.L.F. Armarego, C.L.L. Chai, Purification of Laboratory Chemicals, fifth ed., Butterworth-Heinemann, Elsevier Inc., Amsterdam, The Netherlands, 2003.

[49] S. Celedón, P. Hamon, V. Artigas, M. Fuentealba, S. Kahlal, D. Carrillo, J.-Y. Saillard, J.-R. Hamon, C. Manzur, Ferrocene functionalized enantiomerically pure Schiff bases and their Zn(II) and Pd(II) complexes: a spectroscopic, crystallographic, electrochemical and computational investigation, New J. Chem. 46 (2022) 3948-3960. DOI: 10.1039/D1NJ06106B

[50] G.A. Bain, J.F. Berry, Diamagnetic Corrections and Pascal's Constants, J. Chem. Educ. 85 (2008) 532-536. DOI: 10.1021/ed085p532

[51] APEX2, Bruker AXS Inc., Madison, Wisconsin, USA, 2007.

[52] O.V. Dolomanov, L.J. Bourhis, R.J. Gildea, J.A.K. Howard, H. Puschmann, OLEX2: a complete structure solution, refinement and analysis program, J. Appl. Crystallogr. 42, (2009) 339-341. DOI: 10.1107/S0021889808042726

[53] G.M. Sheldrick, A short history of SHELX, Acta Crystallogr. Sect. A 64 (2008) 112-122. DOI: 10.1107/S0108767307043930

[54] H. Le Bozec, T. Le Bouder, O. Maury, A. Bondon, I. Ledoux, S. Deveau, J. Zyss, Supramolecular octupolar self-ordering towards nonlinear optics, Adv. Mater. 13 (2001) 1677-1681. DOI: 10.1002/1521-4095(200111)13:22%3C1677::AID-ADMA1677%3E3.0.CO;2-J

[55] G. te Velde, F.M. Bickelhaupt, E.J. Baerends, C. Fonseca Guerra, S.J.A. van Gisbergen, J.G. Snijders, T. Ziegler, Chemistry with ADF, J. Comput. Chem. 22 (2001) 931-967. DOI: 10.1002/jcc.1056

[56] ADF 2020.1, SCM, Theoretical Chemistry, Vrije Universiteit, Amsterdam, The Netherlands, http://www.scm.com.

[57] E. van Lenthe, E.J. Baerends, J.G. Snijders, Relativistic total energy using regular approximations, J. Chem. Phys. 101 (1994) 9783-9792. DOI: 10.1063/1.467943

[58] J.P. Perdew, K. Burke, M. Ernzerhof, Generalized Gradient Approximation Made Simple, Phys. Rev. Lett. 77 (1996) 3865-3868. DOI: 10.1103/PhysRevLett.77.3865

[59] C. Adamo, V. Barone, Toward reliable density functional methods without adjustable parameters: The PBE0 model, J. Chem. Phys. 110 (1999) 6158-6170. DOI: 10.1063/1.478522

[60] E. Van Lenthe, E.J. Baerends, Optimized Slater-Type Basis Sets for the Elements 1-118, J. Comput. Chem. 24 (2003) 1142-1156. DOI: 10.1002/jcc.10255

[61] S. Grimme, S. Ehrlich, L. Goerigk, Effect of the damping function in dispersion corrected density functional theory, J. Comput. Chem. 32 (2011) 1456-1465. DOI: 10.1002/jcc.21759

[62] J.S. Danilova, S.M. Avdoshenko, M.P. Karushev, A.M. Timonov, E. Dmitrieva, Infrared spectroscopic study of nickel complexes with salen-type ligands and their polymers, J. Mol. Struct. 1241 (2021) 130668. DOI: 10.1016/j.molstruc.2021.130668

[63] D. Lin-Vien, N.B. Colthup, W.G. Fateley, J.G. Grasselli, The Handbook of Infrared and Raman Characteristic Frequencies of Organic Molecules, Elsevier, 1991. ISBN 978-0-12-451160-6

[64] M.A. Al-Anber, Electrochemical behaviour and electronic absorption of the metal β-diketonates complexes, Am. J. Phys. Chem. 2 (2013) 1-7. DOI: 10.11648/j.ajpc.20130201.11

[65] J. Cisterna, V. Artigas, M. Fuentealba, P. Hamon, C. Manzur, V. Dorcet, J.-R. Hamon, D. Carrillo, Nickel(II) and copper(II) complexes of new unsymmetrically-substituted tetradentate Schiff base ligands: Spectral, structural, electrochemical and computational studies, Inorg. Chim. Acta 462 (2017) 266-280. DOI: 10.1016/j.ica.2017.04.001

[66] O. Kahn, Molecular Magnetism, Dover Publications, Garden City, New York, 2021.

[67] J.D. Dunitz, L.E. Orgel, A. Rich, The crystal structure of ferrocene, Acta Crystallogr. 9, (1956) 373-375. DOI: 10.1107/S0365110X56001091

[68] L. Yang, D.R. Powell, R.P. Houser, Structural variation in copper(I) complexes with pyridylmethylamide ligands: structural analysis with a new four-coordinate geometry index, s_4, Dalton Trans. (2007) 955-964. DOI: 10.1039/b617136b

[69] J. Cisterna, V. Dorcet, C. Manzur, I. Ledoux-Rak, J.-R. Hamon, D. Carrillo, Synthesis, spectral, electrochemical, crystal structures and nonlinear optical properties of unsymmetrical Ni(II) and Cu(II) Schiff base complexes, Inorg. Chim. Acta 430 (2015) 82-90. DOI: 10.1016/j.ica.2015.02.030

[70] R. Taylor, P.A. Wood, A Million Crystal Structures: The Whole Is Greater than the Sum of Its Parts, Chem. Rev. 119 (2019) 9427-9477. DOI: 10.1021/acs.chemrev.9b00155

[71] D. Astruc, Electron Transfer and Radical Reactions in Transition-Metal Chemistry, VCH, New York, 1995, ch. 2, pp. 89-195. ISBN 1-56081-566-3

[72] A. Trujillo, M. Fuentealba, D. Carrillo, C. Manzur, I. Ledoux-Rak, J.-R. Hamon, J.-Y. Saillard, Synthesis, Spectral, Structural, Second-Order Nonlinear Optical Properties and Theoretical Studies On New Organometallic Donor-Acceptor Substituted Nickel(II) and Copper(II) Unsymmetrical Schiff-Base Complexes, Inorg. Chem. 49 (2010) 2750-2764. DOI: 10.1021/ic902126a

[73] J.L. Oudar, Optical nonlinearities of conjugated molecules. Stilbene derivatives and highly polar aromatic compounds, J. Chem. Phys. 67 (1977) 446-457. DOI: 10.1063/1.434888

[74] S. Celedón, T. Roisnel, D. Carrillo, I. Ledoux-Rak, J.-R. Hamon, C. Manzur, Transition metal(II) complexes featuring push-pull dianionic Schiff base ligands:Synthesis, crystal structure, electrochemical and NLO studies, J. Coord. Chem. 73 (2020) 3079-3094. DOI: 10.1080/00958972.2020.1827237

[75] J. Xu , S. Semin , T. Rasing , A.E. Rowan, Organized Chromophoric Assemblies for Nonlinear Optical Materials: Towards (Sub)wavelength Scale Architectures, small 2015, 11, 1113-1129. DOI: 10.1002/smll.201402085